Metabolomics Study of Dried Ginger Extract on Serum and Urine in Blood Stasis Rats Based on UPLC-Q-TOF/MS

Min Su
Anhui University of Traditional Chinese Medicine
Gang Cao
Zhejiang Chinese Medical University
Xiaoli Wang
Anhui University of Traditional Chinese Medicine
Raftery Daniel
University of Washington
Yan Hong
Anhui University of Traditional Chinese Medicine
yanquan Han (327807538@qq.com)

Research

Keywords: Dried ginger, Blood stasis syndrome, UPLC-Q-TOF/MS, Metabolomics

Posted Date: May 29th, 2020

DOI: https://doi.org/10.21203/rs.3.rs-31241/v1

Abstract

Backgroud: According to the theory of traditional Chinese medicine (TCM), blood stasis syndrome (BSS) is the basis for many cardiovascular diseases. Ginger is often used as Chinese medicine (herb medicine) in China and Southeast Asia for the treatment of cardiovascular, respiratory, and digestive diseases. but the specific mechanism is unclear.

Methods: After establishing an acute rat model of blood stasis syndrome, blood and urine of 5 groups of rats were collected for analysis of efficacy indicators. Aortic vessels are used for pathological testing. Serum and urine were used for metabolomics, multivariate statistical analysis was used to explore metabolites and metabolic pathways, and the correlation between metabolites and pharmacodynamic indicators was further explored.

Results: In this experiment, the model of blood stasis syndrome was successfully established based on changes in vascular disease and the efficacy index. The experimental results show that the efficacy indicators of dried ginger (DG) extracts of different doses have different degrees of changes than model group (MG), and the high dose of dried ginger group (GJH) changes are the most significant ($p < 0.05$ or $p < 0.01$). And 22 metabolites (10 in serum and 12 in urine) were identified and contributed to the blood stasis progress. These metabolites mainly involve seven metabolism pathways in different impact-value. Dried ginger has therapeutic effects on BSS rats by regulating multiple metabolic pathways.

Conclusion: This study provides an effective method for understanding the metabolic mechanism of dried ginger extracts on BSS.

Backgroud

Cardiovascular disease is a significant cause of death worldwide, accounting for about 30% of global deaths [1]. BSS is a common disease, which is closely related to many diseases, such as coronary heart disease, infertility, and cancer [2]. Blood stasis is a complex pathological system, usually accompanied by vascular endothelial injury, inflammation, liver and kidney injury, and other symptoms, which further promote the occurrence of blood stasis [3, 4]. In modern medicine, the cognition of BSS mainly refers to insufficient blood circulation, decreased blood flow to the body, or impurities in the blood [5]. The pathological indexes of BSS include hemorheology, coagulation function, and so on [6]. In Chinese medicine research, the treatment of BSS by TCM has received widespread attention due to its unique advantages.

Ginger (Zingiber officinale Rosc.) is taxonomically characterized as perennial, aromatic, tuberous, and non-tuberous rhizomes [7]. Mainly produced in China, India, and other places and used as food seasoning ingredients and medicinal resources, especially for the treatment of diseases related to inflammation and oxidative stress [8–12]. Ginger is rich in phytochemicals, such as gingerols, shogaols, and zingerone [13]. In recent years, ginger has attracted increasing attention due to its pharmacological properties, such as its anti-inflammatory, anticarcinogenic, and antioxidant activities [14–16]. In our country, Ginger is a commonly used medicinal and food dual-use traditional Chinese medicine, which was first published in Shennong Bencao Jing. It has a long history of medicinal use and significant clinical efficacy [17]. DG has the effects

of warming blood and activating blood, warming the lungs, reduce cough and suppress vomiting, modernly used to treat heart failure, cold cough, vomiting, tumors, etc. Moreover, studies have shown that ginger can improve hemorheology events, inhibit platelet aggregation, prevent thrombosis, play an anticoagulant role [18, 19]. However, the understanding of its treatment of BSS is limited, and this is a problem worthy of our attention.

Metabolomic is a scientific technology for quantitative measurement of the time-related multiparametric metabolic response of multicellular systems to pathophysiological stimuli or genetic modification [20], which provides a unique chemical fingerprint of a specific organism and reveals the essence of the syndrome and the therapeutic effect of Chinese medicine, it involves “holistic-dynamic-comprehensive analysis” [21]. High-throughput metabolomics analysis has been used to reveal metabolic profiles. Owing to the massive amount of accurate chemical data, high-speed data acquisition, and high resolution, UPLC-Q-TOF/MS based metabolomics has been widely used in dynamic analyses of biochemical changes during drug intervention, which is useful for elucidating intervention mechanisms [22, 23]. Combined with multivariate data analysis, the metabolic profiles of each intervention group or NG can be visually displayed, and endogenous metabolites with significant differences between groups can be identified as biomarkers [24].

In this study, we established an clinical rat model of acute BSS ,collected serum and urine samples from each group. UPLC-Q-TOF/MS combined with multivariate statistical analysis of serum and urine was used to conduct multi-dimensional analysis on the metabolic spectrum, and to explore the changes of its metabolites.

Methods

Chemical and reagents

Methanol and acetonitrile were purchased from Dikma Technologies Inc (Beijing,USA); Ultrapure water was prepared by a Milli-Q water purification system(Millipore, Bedford, MA, USA);The reference substance are as follows: 6-gingerol, 8-gingerol, 10-gingerol, 6-shogaol were bought from Chengdu Munster Biotechnology Co., Ltd., with 98.79%, 98.81% and 99.13%, 98.79% purity, respectively. All the other chemicals and biochemical used are of the highest grade available. Hemorheological reagent, Mass spectrometry reagent, MS grade formic acid was purchased from Sigma-Aldrich (St. Louis, MO, USA). The coagulometer (SYSMEXCA7000) was produced by Sysmex, Japan. PT, APTT, TT, FIB quality control plasma N.P are all Sysmex products. DG (Lot No. 201804072) was obtained from the pharmacy of the First Affiliated Hospital of Anhui University of Chinese Medicine and was identified as ginger by Professor Peng Huasheng (College of Pharmacy, Anhui University of Chinese Medicine).

Extraction and content identification of DG

In brief, 1.0 kg of rhizome was decocted for 40 min with10 times distilled water repeatedly for two times. The decoctions were collected, mixed, filtered, concentrated under reduced pressure, and dried by vacuum at 75℃. The w/w yields of DG were 11.74%. The DG extract was re-dissolved in distilled water to a final

concentration of 2 g/mL (equivalent to the dry weight of crude drugs) before being used. And further analyzed with a Waters Acquity H-Class UPLC equipped with an Acquity BEH C18 column (100 mm × 2.1 mm with the particle size of 1.7 μm), which consisted of a photodiode array detector, and the mobile phase was comprised of acetonitrile (A) and water (B). The gradient mode was as follows: initial 3% A linear gradient to 85% A in 10.0 min; linear gradient to 100% A in 15.0 min; 100% B from 15.0–18.0 min, 100–3% A over 18.0–20.0 min and final wash at 3% A over 20–22 min. The flow rate was 0.3 mL/min. The detector wavelength was set at 280 nm.

Animals treatment

Male SD rats weighing 200–220 g were purchased from the Animal Center of Anhui Medical University. They were kept in plastic cages at 25 ± 2℃ with free access to pellet food and water and on a 12 h light / dark cycles. Animal welfare and experimental procedures were carried out following the guidelines for the care and use of laboratory animals (National Research Council of USA,996).

Experimental model and drug administration

A total of 60 SD rats were randomly divided into five groups equally, including NG, MG, GJH, GJM, GJL (DG extract, 2.10, 1.05, 0.53 g/kg, respectively). TCM intervention groups were orally administered different doses of DG extract, respectively, and the control group was orally administered an equivalent volume of distilled water. BSS was induced by placing the rats of the model and TCM intervention groups in ice water (0–2℃) for 5 min daily for 14 consecutive days. After that, all groups except for NG were injected with 0.8 ml kg^{-1} adrenaline hydrochloride twice with an interval of 4 h. After the first injection, rats were immersed in ice water (0–2℃) for swimming for 5 min. Rats fasted overnight, and the administration of DG extract was continued after performing the model. Blood samples were collected on the following day at 40 min after the last administration.

Sample collection

Urine samples were taken from six rats in each group between 18–24 h after the second injection of epinephrine, and the rats was anesthetized with pentobarbital (50 mg narcoren / kg body weight) at 24 h after the last injection of Adr, stored at -80℃ before analysis. Serum was isolated by centrifugation at 3500 rpm for10 min at 4℃ and then frozen − 80℃ before metabolomics detection. Then the Other rats were anesthetized by intraperitoneal injection of pentobarbital (50 mg narcoren / kg body weight) 1 hour after the administration on the second day. The blood collection was carried out by carotid artery intubation, and the anticoagulation was carried out at the ratio of 1:9 with 3.8% sodium citrate. The whole blood viscosity, plasma viscosity, and clotting time were measured using a fully automatic hemorheometer. The blood samples of the remaining six rats in each group were drawn from the abdominal aortic to determine hemorheological variables. Blood was collected into plastic tubes with 3.8% sodium citrate for plasma anticoagulation and detected for WBV, ESR, and PCV. Then plasma was separated from blood by centrifugation at 3500 rpm for 10 min and detected for PV and plasma anticoagulation. All experiments were completed within 4 h after blood collection.

Viscosity determination

A total of 800 μL blood or plasma was used to determine the viscosity with a one-plate viscometer (Model LG-R-80B, Steellex Co., China) at different shear rates maintained at 37℃. WBV was measured with shear rates' varying from 1 to 200/S. PV was measured at the high shear rate (200/S) and low shear rate (50/S). ESR and PCV measurements are a total of 1000μL blood that was put into an upright Westergren tube. The rate of red blood cells falling to the bottom of the tube (mm per hour) was observed and reported. The volume of packed red blood cells was immediately measured in the tube after centrifugation (3000 rpm for 30 min). TT, PT, APTT, and FIB were examined with commercial kits following the manufacturer's instructions by a coagulometer (Model LG-PABER-I, Steellex Co., China). TT was determined by incubating 50 μL plasma solutions for 3 min at 37℃, followed by the addition of 100 μL thrombin agent. PT was determined by incubating 50 μL plasma solutions for 3 min at 37℃, followed by the addition of 100 μL thromboplastin agents. APTT was determined by incubating 50 μL plasma with 50 μL APTT-activating agent for 3 min at 37℃, followed by addition of 50 μL CaCl2. FIB was determined by incubating 10 μL plasma with 90 μL imidazole buffers for 3 min at 37℃, followed by addition of 50℃ FIB agent. The anticoagulation activity was assessed by assaying the prolongation of the plasma clotting time of TT, APTT, increase INR of PT, and reduction of FIB content (Sysmex CA7000, Japan).

Preparation of metabolomic samples

Before analysis, the 200 μL aliquot of serum samples was thawed at 4℃, and then 600 μL methanol to precipitate the proteins. Vortex the mixture for 1 minute and centrifuged at 14,000 rpm for 15 min at 4℃. The supernatant (600 μL) was transferred to the EP tube and evaporated to dryness at 4℃ under a stream of nitrogen. Dissolve the residue with 200 μL methanol followed by vortexing for 60 s and centrifuged at 14000 rpm for 5 min. Transfer the supernatant (80 μL) to auto-sampler vials for UPLC-Q-TOF/MS analysis. The processing of urine is the same as that of serum samples. Pooling aliquots prepared a QC sample from all samples collected in the course of the study. A pooled QC sample was made by mixing aliquots (20 μL) of each sample and handled by the same method as the samples. The pooled QC sample was analyzed randomly through the analytical run to monitor instrument stability. Besides, a random sample is split into six parts and processed in the same way. These six samples were continuously analyzed injected to validate the repeatability of the sample preparation method.

UPLC–Q-TOF/MS conditions

Perform serum or urine metabolic profiling on UPLC-Q-TOF/MS system coupled to a Waters Q-Tof Premier Mass Spectrometer. Perform urine and serum chromatography on a Waters Acquity UPLC BEH C_{18} column (2.1 × 100 mm, 1.7 μm) with the temperature of the column set at 30℃. The flow rate was 0.3 mL/min^{-1} and the mobile phase was ultrapure water with 0.1% formic acid (A) and acetonitrile (B). The gradient elution procedure is as follows: 0–1 min, 1% ◊ 10% B;1–2 min,10% ◊ 30% B□2–4 min□30% ◊ 75% B□4–7 min□75% ◊ 75% B□7–9 min□75% ◊ 100% B□9–11.5 min□100% ◊ 100% B□11.5–12 min□100% ◊ 1% B□12–13.5 min□1% ◊ 1% B. Sample analysis time was 13.5 min, and the sample injection volume was 2 μL. The auto-sampler maintained at 4℃. The ESI source has two working modes: positive and negative patterns. The quality test parameters are set as follows: The N_2 flow rate is set to 650 L/h, and the positive and negative ion mode is 600 L/h, respectively; The gas temperature was 350℃; The source temperature was set to 110℃, with a cone gas flow of 100 L/h. The capillary voltage was set at 1.5 kV in positive ion mode,

and 1.8 kV in negative ion mode and the sample cone voltage was set at 100 V. All sample detections were acquired by using the lock-spray to ensure accuracy and reproducibility. A lock-mass at a concentration of 200 pg/mL was employed via a lock-spray interface. The MS/MS analyses of the ions were performed at different collision energy parameters that ranged from 5 and 50 eV for plasma samples and from 10 and 50 eV for the urine samples. The ESI interface was used, and the profile data were collected in full scan mode from m/z 50–1000. Leucine-enkephalin was used as the lock-mass reference compound (m/z 556.2771 in positive mode□m/z 554.2615 in negative mode) and the flow rate was 20 μL /min.

Data processing and analysis

The mass data acquired were imported to Markerlynx XS (Waters Corporation, MA, USA) within the Masslynx software for peak detection and alignment. The original data were processed using the following parameters: the retention time range was 0–13 min, the mass range was 50–1000 Da, the retention time tolerance was 0.01 min, and the mass tolerance was 0.1 Da. Multivariate statistical analysis in the form of PLS-DA and OPLS-DA was performed using pareto-scale data. Extract potential biomarkers from S-maps constructed by OPLS-DA analysis, and VIP is also used to select potential biomarkers. V ariable importance in projection (VIP) score > 1 and t-test P value < 0.05 were prerequisite conditions for biomarkers. PCA, OPLS-DA, clustering heatmap analysis, correlation analysis, relative intensity analysis, and pathway analysis with MetaboAnalyst 4.0 (http://www.metaboanalyst.ca/). Other statistical analyses were performed using SPSS 22.0, and the experimental data were expressed as the mean ± SD. Comparisons between groups were performed using one-way analysis of variance (ANOVA). Bilateral P values less than 0.05 were considered statistically significant.

Through the identification of biomarkers and the construction of metabolic pathways, research was conducted on essential ions found from statistical analysis to determine whether they provided potential biomarkers. These ions were tentatively identified based on their m/z value and mass spectrum using inhouse data. More specifically, the following web-based search engines were also used to provide potential identities for these ions: Human Metabolome Database (http://www.hmdb.ca/), MassBank (http://www.massbank.jp/), and ChemSpider database (www.chemspider.com). The construction, interaction, and pathway analysis of potential biomarkers was performed with IPA (http://metpa.metabolomics.ca./ MetPA/faces/Home.jsp) based on database source including the KEGG database (http://www.genome.jp/kegg/), the Human Metabolome Database (http://www.hmdb.ca/), SMPD (http://www.smpdb.ca/), and METLIN (http://metlin.scripps.edu/). The possible biological roles were evaluated by the enrichment analysis using the MetaboAnalyst, which is a web-based tool for visualization of metabolomics.

Results

Content determination results of DG

The components were identified and quantified by comparison of retention time and calculation of peak areas from the chromatograms with those of known standards. DG extract contained determine 6-gingerol, 8-gingerol, 6-shogaol and 10-gingerol were 6.95,0.99,0.42 and 1.32 mg/g, respectively (Fig. 1).

Pathological observation of vascular

The microstructures of the abdominal aorta in rats was observed. Vascular obstruction and a small amount of micro thrombosis were observed in the MG. Some endothelial cells fell off from the vascular wall, endothelial cells swelled, and intima thickened. Also, inflammatory cell infiltration was observed. The above pathological symptoms were alleviated in the administration group, especially in the GJH (C). The results are shown in Figure S1.

Effect of DG on blood viscosity

The impact of WBV is shown in Fig. 2 and Table S1. In the MG of BSS, WBV increased significantly at all shear rates. After administration, the WBV of each group was significantly reduced at high shear rates ($p < 0.01$ or 0.05). And the table also shows the effects of DG on plasma viscosity. The model rats had a significantly higher plasma viscosity than the controls. The plasma viscosity in the GJH, GJM, GJL was significantly decreased compared to the MG ($p < 0.01$ or 0.05).

Effect of DG on ESR, PCV, DI and EAI

The results of ESR, PCV, EAI, and DI for each group are shown in Table 1. All four indexes were significantly higher in the MG than in the NG. GJH, GJM are reduced ESR and PCV ($P < 0.05$). All DG dose groups decreased DI and EAI ($P < 0.05$ or $P < 0.01$).

Table 1
Effect of DG extract on ESR, PCV, DI, and EAI

Group	Dose(g/kg)	ESR(MM/H)	PCV(%)	DI (%)	EAI
NG	—	3.30 ± 1.15	31.67 ± 7.34	66.17 ± 7.63	2.23 ± 0.40
MG	—	10.37 ± 2.85##	51.83 ± 7.70##	83.83 ± 7.65##	5.24 ± 0.92##
GJH	2.10	6.28 ± 1.06*	39.17 ± 8.11*	71.33 ± 7.39*	3.08 ± 0.65**
GJM	1.05	7.68 ± 0.43*	42.33 ± 6.09*	73.17 ± 8.04*	3.49 ± 0.88**
GJL	0.53	7.90 ± 1.64	44.50 ± 6.89	74.33 ± 6.62*	3.92 ± 0.83*

Data represent mean ± S.D. n = 6. #Compared with NG, $p < 0.05$. ##Compared with NG, $p < 0.01$. *Compared with MG, $p < 0.05$. **Compared with MG, $p < 0.01$.

Effect of DG on plasma coagulation parameters

The impacts of DG on blood coagulation were evaluated by assays of APTT, PT, TT, and FIB in the plasma. PT was decreased, FIB was increased, APTT and TT were significantly shortened in the model rats compared with the NG levels, as showed in Table 2. After administration, compared with the MG, the PT of GJH and GJM was significantly increased, and the FIB was significantly decreased ($P < 0.05$). In terms of TT and APTT, the DG group was significantly longer ($P < 0.05$).

Table 2
Effect of DG extract on Plasma Coagulation Parameters

Group	Dose(g/kg)	PT(INR)	FIB (g)	TT(S)	APTT(S)
NG	—	1.37 ± 0.15	2.11 ± 0.26	48.90 ± 4.70	32.33 ± 5.75
MG	—	0.88 ± 0.21##	6.38 ± 0.79##	30.77 ± 6.30##	20.67 ± 4.41##
GJH	2.10	1.21 ± 0.16*	5.16 ± 1.02*	44.24 ± 5.42**	30.50 ± 8.55*
GJM	1.05	1.16 ± 0.21*	5.33 ± 0.803*	42.53 ± 645*	29.33 ± 7.39*
GJL	0.53	1.00 ± 0.18	5.66 ± 1.08	39.82 ± 5.44*	28.67 ± 7.01*

Data represent mean ± S.D. n = 6. #Compared with NG, $p < 0.05$. ##Compared with NG, $p < 0.01$. *Compared with MG, $p < 0.05$. **Compared with MG, $p < 0.01$.

Metabolic profiling analysis

To obtain the maximum possible information for each metabolite, the experiments were performed in both positive and negative ionization modes, and LC-MS-MS analyzed serum and urine samples under the same chromatographic conditions. The typical total ion chromatograms (TICs) of the serum and urine samples from the NG, MG, and GJH collected in the experiment are presented in Figure S2. To further analyze changes between complex sets of data, the multivariate data analysis techniques, including PCA-X, PLS-DA and OPLS-DA, were used to analyze LC-MS data.

PCA analysis was used to assess the difference in metabolite profiles between serum and urine samples of NG and MG. The apparent separation between them was obtained in the PCA scores plot (Fig. 3A, B), which indicated that the two groups had utterly different metabolic profiling. Then, the PLS-DA method was used to systematically evaluate the metabolomics of BSS rats (permutation number: 200). In PLS-DA, the NG was more distinct from the MG (Fig. 3C, D). The PLS-DA model parameters were as follows: $R^2 = 0.846$ and $Q^2 = -0.0669$ in serum, and $R^2 = 0.831$and $Q^2 = -0.00977$ in urine, which showed an excellent predictive power (Fig. 3E, F). To screen differential metabolites and maximize the discriminatory ability of serum and urine metabolites between the groups, orthogonal partial least squares discriminant analysis (OPLS-DA) was used. As showed in the score plot (Fig. 3G, H), the serum and urine samples in the MG were significantly different from those in the NG. The S-plots (Fig. 3I, J) showed differential metabolites between the two groups, and VIP was obtained based on OPLS-DA with a threshold than 1 would be viewed as potential biomarkers. Combined with the results of the S-plot and VIP-value plot together, the UPLC-Q-TOF/MS analysis platform provided the retention time, precise molecular mass, and MS/MS data for the structural identification of biomarkers. The same procedures were utilized to analyze the plasma samples derived from the NG, GJL, GJM and GJH.

Moreover, we investigated the differences in metabolic profiles between the MG and the GJL, GJM and GJH, using OPLS-DA analysis. Score 3D plots (Figure S3 A, B) from OPLS-DA were used to maximize the discrimination of metabolite differences among the five groups. The figure shows that the metabolites of serum and urine in GJL, GJM, and GJH gradually approach the NG. Meanwhile, the GJH was the closest to

the NG, the GJL was the closest to the MG, and the GJM was between the GJH and the GJL. Therefore, the intervention of DG on endogenous metabolites in rats with BSS shows a significant dose-effect relationship.

Biomarker identification

To select potential biomarkers related to BSS, the first principal component of VIP was obtained. Firstly, the VIP values greater 1.0 are selected as changing metabolites. And then, the remaining variables were calculated by Student's t-test (t-test), $P < 0.05$, variables are discarded between two comparison groups. Besides, several commercial databases, such as HMDB (http://www.hmdb.ca), KEGG (http://www.kegg.jp) and NIST (http://www.nist.gov/index.html), were used for searching the information of metabolites.

The retention time, precise molecular mass, and MS/MS data was provided for the structural identification of potential biomarkers using the analysis platform of EZ-info software. The accurate molecular mass was detected within 5 ppm in measurement errors by TOF. Meanwhile, the potential elemental composition, the degree of unsaturation and the fractional isotope abundance of compounds were obtained. The supposed molecular formula was searched in ChemSpider, the Human Metabolome Database, Mass Bank, and other relevant databases were used to identify the possible chemical constitutions, and MS/MS data were screened to determine the potential structures of the ions. Details of potential biomarkers were listed in Table 3.

Table 3
Potential biomarkers in serum and urine

	NO	RT	Formula	Metabolites	VIP	P	FC
Serum	1	0.6595	$C_3H_4O_3$	Pyruvate	1.0050	0.0024	0.6187
	2	0.9963	$C_{15}H_{12}O$	Chalcone	2.4297	0.0031	2.9408
	3	1.4248	$C_{29}H_{50}O_4$	6-Deoxohomodolichosterone	1.4195	0.0091	2.0295
	4	2.2860	$C_{18}H_{29}NO_2$	Penbutolol	1.2444	0.0190	1.9356
	5	3.8942	$C_{18}H_{39}NO_3$	Phytosphingosine	1.2193	0.0367	1.6779
	6	6.4867	$C_{20}H_{41}NO_3$	Ethanolamine Oleate	1.4903	0.0068	2.1090
	7	7.6357	$C_{16}H_{24}N_2O$	Oxymetazoline	1.2449	0.0004	1.7684
	8	7.6965	$C_{19}H_{38}O_4$	1-Monopalmitin	1.6229	0.0172	2.1786
	9	8.5343	$C_{47}H_{76}O_2$	α-calendic acid	1.0186	0.0054	1.6551
	10	14.0018	$C_{14}H_{11}NO$	Phosphonoacetaldehyde	1.7977	0.0004	2.2653
Urine	1	0.7043	$C_{14}H_{11}NO$	3-Methyl-9H-carbazole-9-carboxaldehyde	1.3875	0.0359	0.6445
	2	2.7173	$C_{22}H_{32}N_2O_5$	Benzquinamide	1.7277	0.0001	0.3362
	3	0.6694	$C_3H_7NO_2$	L-Carnitine	1.4923	0.0291	0.2745
	4	0.6896	$C_4H_9N_3O_2$	L-Alanine	1.9506	0.0049	0.0529
	5	0.6898	$C_6H_8N_2O_2$	Creatine	1.9488	0.0063	0.0536
	6	0.7301	$C_9H_{13}N_3O_3$	L-isoleucyl-L-proline	1.5086	0.0078	0.3532
	7	1.2144	$C_5H_7N_3O$	5-Methylcytosine	1.3817	0.0400	2.8193
	8	1.7440	$C_{17}H_{22}N_2O_7$	Tetrahydropentoxyline	1.5986	0.0180	1.6918
	9	3.1393	$C_{11}H_{19}NO_{10}S_2$	Progoitrin	1.5839	0.0082	2.6975
	10	3.1389	$C_{11}H_{19}O_{13}P$	1-Phosphatidyl-D-myo-inositol	1.4146	0.0160	2.8472
	11	9.6106	$C_{20}H_{41}NO_3$	Ethanolamine Oleate	1.8239	0.0291	2.8580
	12	9.7938	$C_{24}H_{40}O_6$	3b,4b,7a,12a-Tetrahydroxy-5b-cholanoic acid	1.8367	0.0104	2.1858

Metaboanalyst 4.0 (www.metaboanalyst.ca/) is used for pathway construction by employing the rice metabolic pathway databases as reference for the global test algorithm. Table 4 shows the identified biomarkers and their trends compared with the NG.

Table 4
Summary of intensity values of potential biomarkers in each group

Matrix	Biomarkers	NG	MG	GJH	GJM	GJL
Serum	Pyruvate	2054.53 ± 219.28	3540.26 ± 309.4##	2898.62 ± 421.27	1941.29 ± 287.40**	2406.15 ± 576.39**
	Chalcone	1190.27 ± 311.07	49.73 ± 166.64##	933.49 ± 107.79	765.78 ± 125.21	655.97 ± 148.81
	6-Deoxohomodolichosterone	1459.10 ± 45.85	784.27 ± 132.91##	1166.24 ± 315.19*	1047.37 ± 371.41*	903.75 ± 145.43
	Penbutolol	1379.69 ± 485.53	783.49 ± 141.84##	1170.86 ± 271.58	1066.08 ± 252.95	936.82 ± 164.42
	Phytosphingosine	29605.10 ± 5830.21	19138.72 ± 4393.29#	25570.68 ± 4553.94	23926.42 ± 3939.20	22274.01 ± 4349.25
	Ethanolamine Oleate	4826.64 ± 1381.75	2523.15 ± 689.70#	3780.75 ± 792.81	3368.81 ± 72.566	2757.25 ± 613.47
	Oxymetazoline	2107.08 ± 130.59	1286.33 ± 265.67##	1929.20 ± 245.88**	1657.12 ± 477.21**	1605.2 ± 221.02**
	1-Monopalmitin	2564.01 ± 864.06	1280.57 ± 476.87##	2093.21 ± 466.46	1977.15 ± 55.80	1518.93 ± 490.59
	α-calendic acid	965.48 ± 145.78	643.90 ± 97.28##	894.87 ± 103.88*	714.86 ± 564.18	668.67 ± 59.73
	Phosphonoacetaldehyde	7118.85 ± 675.99	3403.62 ± 1038.04##	5999.82 ± 1260.77**	5202.67 ± 1139.99*	4360.61 ± 1204.03
Urine	3-Methyl-9H-carbazole-9-carboxaldehyde	434.90 ± 136.45	728.62 ± 191.06##	455.14 ± 108.99**	448.74 ± 84.66**	539.19 ± 79.05**
	Benzquinamide	406.17 ± 153.89	1241.39 ± 162.91##	583.35 ± 235.36**	643.73 ± 334.58*	717.24 ± 436.52**
	L-Carnitine	619.78 ± 189.29	2592.49 ± 1115.51#	999.14 ± 250.12	1164.39 ± 514.70	1278.23 ± 478.98

#Compared with NG, $p < 0.05$. ##Compared with NG, $p < 0.01$. *Compared with MG, $p < 0.05$. **Compared with MG, $p < 0.01$.

Matrix	Biomarkers	NG	MG	GJH	GJM	GJL
	L-Alanine	115.75 ± 57.41	2866.42 ± 501.03##	1011.66 ± 151.37	1382.45 ± 603.93	1876.80 ± 939.28
	Creatine	559.21 ± 208.48	13492.18 ± 5090.32##	4305.16 ± 1336.07	5777.50 ± 1179.57	5987.95 ± 1430.89
	L-isoleucyl-L-proline	1635.24 ± 725.09	5166.35 ± 1748.43#	2102.71 ± 1215.84	3787.50 ± 1260.69	4485.61 ± 1489.07
	5-Methylcytosine	3626.66 ± 1238.58	1150.50 ± 609.22##	3107.05 ± 944.98**	2765.35 ± 1441.79*	1767.78 ± 541.37**
	Tetrahydropentoxyline	1645.85 ± 737.43	944.80 ± 104.29#	1772.12 ± 655.85	1247.53 ± 557.70	1020.69 ± 139.07
	Progoitrin	1257.27 ± 413.71	482.18 ± 169.51#	1056.89 ± 463.63	1132.06 ± 402.24**	954.89 ± 334.78**
	1-Phosphatidyl-D-myo-inositol	1017.94 ± 622.52	355.60 ± 143.10#	977.23 ± 272.19*	961.55 ± 557.54*	636.25 ± 211.77
	Ethanolamine Oleate	4809.81 ± 853.54	1997.75 ± 626.62##	4761.77 ± 407.20**	3986.53 ± 865.61**	2888.81 ± 251.27**
	3b,4b,7a,12a-Tetrahydroxy-5b-cholanoic acid	1438.69 ± 259.84	735.58 ± 115.77##	1484.81 ± 774.85**	1343.59 ± 575.07**	1164.67 ± 374.06

#Compared with NG, $p < 0.05$. ##Compared with NG, $p < 0.01$. *Compared with MG, $p < 0.05$. **Compared with MG, $p < 0.01$.

Metabolic Pathway Analysis

Possible ways to further explore the effects of BSS, using online MetaboAnalyst 4.0 software (www.metaboanalyst.ca), through the analysis of blood and urinary tract, found seven pathways affected (Fig. 4) in the BSS, these ways include arginine and proline metabolism, citrate cycle (TCA cycle), pyruvate metabolism, glycolysis/gluconeogenesis, phosphatidylinositol signaling system, inositol phosphate metabolism, and glycerophospholipid metabolism. Pathways with an impact value > 0.1 were considered to be the most important pathways. The results showed that pyruvate metabolism (Impact value = 0.21) and glycolysis/gluconeogenesis (Impact value = 0.10) and phosphatidylinositol signaling system (Impact value = 0.10) were the most important pathways for the development of BSS.

Correlation analysis between biomarkers and pharmacology Indicators

A correlation map of rat serum and urine metabolites of biomarkers and pharmacological indicators of BSS was conducted based on Pearson's correlation coefficients. The correlation heatmap in Fig. 5, shows that the metabolites of Sm1 (serum, Pyruvate), Um1 (urine,3-Methyl-9H-carbazole-9-carboxaldehyde), Um2 (urine,Benzquinamide), Um3 (urine,L-Carnitine), Um4 (urine,L-Alanine), Um5 (urine,Creatine), Um6 (urine,L-isoleucyl-L-proline) were positive related to the level of WBV1, WBV5, WBV30, WBV50, WBV200,PV, ESR, PCV, DI, EAI, FIB, and they are negatively correlated with PT, TT and APTT. However, the correlation of pharmacological indicators corresponding to Sm2(serum, Chalcone), Sm3 (serum, 6-Deoxohomodolichosterone), Sm4 (serum, Penbutolol), Sm5(serum, Phytosphingosine), Sm6 (serum, Ethanolamine Oleate), Sm7 (serum, Oxymetazoline), Sm8 (serum, 1-Monopalmitin), Sm9(serum, α-calendic acid), Sm10(serum, Phosphonoacetaldehyde) Um7 (urine, 5-Methylcytosine), Um8 (urine, Tetrahydropentoxyline), Um9 (urine, Progoitrin), Um10 (urine, 1-Phosphatidyl-D-myo-inositol), Um11 (urine, Ethanolamine Oleate), Um12 (urine, 3b,4b,7a,12a-Tetrahydroxy-5b-cholanoic acid), is just the opposite. Among them Sm2 with TT, Sm8 with PT, Um4 with PCV, EAI, Um5 with DI are strongly positively correlated (r = 0.998, 0.998, 0.996, 0.996, 0.999, respectively), Sm2 with WBV1, WBV5, DI, Sm5 with PCV, Sm7 with WBV30, Um2, Um3 with APTT (r=-0.999, -0.999, -0.997, -0.998, -0.998, -0.997, -0.999, respectively), are strongly negatively correlated. These correlations may indicate that changes in metabolites are related to changes in metabolites and pharmacological indicators.

Correlation analysis of biomarkers in each group

The heat map (Fig. 6) shows the correlation of 22 potential biomarkers in different groups. These potential biomarkers were up-regulated and down-regulated to different degrees in NG and MG.In addition, the results of hierarchical clustering analysis provide visual visualization of each group, the contents of metabolites Sm1(serum, Pyruvate), Um1(urine, 3-Methyl-9H-carbazole-9-carboxaldehyde), Um2(urine, Benzquinamide), Um3(urine, L-Carnitine), Um4(urine, L-Alanine), Um5(urine, Creatine) and Um6 (urine, L-isoleucyl-L-proline) are decreased, while the contents of other metabolites are increased, while MG and GJL were opposite to NG. It can be seen that GJH and NG metabolism are the most similar, while GJL and MG metabolism are the closest (red: increased; blue: decreased).

Discussion

In this study, UPLC-Q-TOF / MS-based metabonomics was used to compare the effects of DG extracts on BSS. The metabolites of MG and NG were significantly different. In the rat model, a total of 22 metabolites were altered in 7 metabolic pathways, Glycolysis/Gluconeogenesis, phosphatidylinositol signaling system, and Pyruvate metabolism are a critical pathway. In terms of pharmacological indicators, different doses of DG extract have different degrees of improvement in pharmacological indicators. These indicates that changes in metabolites may be related to changes in pharmacological indicators. The correlation analysis of metabolites between different groups showed that different dose of DG extract can regulate metabolic disorders in BSS rats to varying degrees; The comparison of each dose group, it was found that the metabolite content increased or decreased in a dose-dependent, and the metabolite content of the GJH was closest to NG, indicating that GJH had the best efficacy.

Through the study, it was found that BSS model rats showed a certain degree of damage in hemorheology. Each dose group of DG had different protective effects, and the metabolites could be adjusted to the normal level to different degrees. Due to the different contents of its components, each group had a different impact on promoting blood circulation and removing blood stasis, It is dose-dependent. Gingerol has been reported to inhibit inflammatory factors, angiotensin II activity, platelet cyclooxygenase activity, thromboxane synthesis, and advanced glycation end products, promote myocardial sarcoplasmic reticulum Ca^{2+}- ATPase activity, regulate the expression of related enzymes and proteins in the process of blood lipid metabolism and exert cardiovascular pharmacological effects, such as cardiotonic, antiplatelet, hypolipidemic, anti-atherosclerosis [25]. This study can provide a scientific basis for further understanding of the mechanism of activating blood circulation and removing blood stasis by DG.

Glycolysis is a common way for all organisms to extract energy from glucose, and gluconeogenesis provides a source for new glucose molecules. Glucose is produced from small carbohydrate substrates such as pyruvate, lactic acid, glycerin, and glucose amino acids, and to synthesize glucose from simple starting materials to meet the needs of various tissues [26–27]. And In our study, when BSS occurred, the model group showed significant upregulation of pyruvate, suggesting that glucose metabolism disorders may occur. After DG intervention, the pyruvate metabolism of the DG group was different from that in the model group, which indicated that the effect of DG on rats with BSS may involve the regulation of glucose metabolism.

The phosphatidylinositol signaling pathway is the hydrolysis of phosphatidylinositol diphosphate through the cell membrane to produce the double-signaling molecules inositol triphosphate and glycerol diester, the formation of which in many cases requires the simultaneous involvement of IP3-Ca^{2+} and DAG/PKC two different signaling pathways [28]. It has been reported that the phospholinositol signaling pathway plays a key role in inhibiting the apoptosis of vascular endothelial cells [29]. In our study, it was found that 1-phosphoatidyl-d-myo-inositol was significantly down-regulated in the MG when BSS occurred, suggesting that vascular endothelial cell abnormalities may occur. After DG intervention, there was a significant difference between the DG group and MG, suggesting that the effect of DG on rats with blood stasis may be related to the phosphatidylinositol signaling system.

Pyruvate can stimulate the transcription of fibroblast growth factor receptors and vascular endothelial growth factor m RNAs and promote the aggregation of new blood vessels in tissues. Studies have shown that pyruvate can reduce intestinal ischemia-reperfusion injury (IRI) and effectively protect internal organs by shortening hypoxemia time, removing oxygen free radicals, inhibiting inflammatory response, increasing pH value and increasing energy production [30]. In this study, compared with the NG, the metabolic pathway of pyruvate in the MG was destroyed, and pyruvate was abnormally increased, indicating that pyruvate level was increased under the condition of disease, and there were differences between the other groups and the MG.

Conclusions

In this study, UPLC-Q-TOF/MS metabolomics and multivariate statistical analysis were used to compare the efficacy of different doses of DG extract on BSS. Through the research of metabolites in rats with BSS, it was found that 22 metabolites in rats with BSS had significant metabolic differences, which may be potential biomarkers or therapeutic targets in the development of BSS. The effect of DG on BSS may be related to the regulation of Glycolysis/ Gluconeogenesis, phosphatidylinositol signaling system, and Pyruvate metabolism. In addition, we found that DG has a dose-dependent increase or decrease in the metabolism of BSS, these findings reveal the possible mechanism of action of DG in the treatment of BSS. Therefore, this study also provides a basis for exploring DG as an alternative drug for treating blood stasis syndrome, however, the specific mechanism is not clear, and future studies are needed to investigate the potential roles of DG in the regulation of the selected endogenous metabolites associated with BSS.

Abbreviations

DG: dried ginger; UPLC-Q-TOF/MS: ultra-high-performance liquid chromatography-quadrupole-time of flight mass spectrometry; SD: Sprague–Dawley; BSS: blood stasis syndrome; TCM: traditional Chinese medicine; NG: normal group; MG: model group; GJH: high dose of dried ginger group; GJM: middle dose of dried ginger group; GJL: low dose of dried ginger group; i.p: intraperitoneal injection; WBV: whole blood viscosity; ESR: erythrocyte sedimentation rate blood; PCV: packed cell volume; PV: plasma viscosity; TT: thrombin time; PT: prothrombin time; APTT: activated partial thromboplastin time; FIB: fibrinogen content; QC: quality control; ESI: electrospray ionization; N_2: dry gas; PLS-DA: partial least-squares discriminant analysis; OPLS-DA: orthogonal partial least squares discriminant analysis; VIP: variable importance in prediction; PCA: principal component analysis.

Declarations

Conflicts of Interest

The authors declare that they have no competing interests.

Acknowledgements

Not applicable

Consent for publication

Not applicable.

Author contributions

MS carried out the main experiments and drafted this manuscript. GC and DR participated in metabonomics research and data analysis. XLW completed the determination and analysis of UPLC. YH designed part of the efficacy experiment and revised the manuscript. YQH directed the experimental research and manuscript writing. All authors read and approved the final manuscript.

Author details

[1]Grade Three-level Laboratory of TCM Preparation, State Administration of Traditional Chinese Medicine /Anhui Province Key Laboratory of Chinese Medicinal Formula (Anhui University of Chinese Medicine) /Engineering Technology Research Center of Modernized Pharmaceutics, The First Affiliated Hospital of Anhui University of Chinese Medicine, Hefei 230031, China. [2]Zhejiang Chinese Medical University. [3]Anhui University of Chinese Medicine, Hefei 230031, China. [4]Northwest Metabolomics Research Center /Mitochondria and Metabolism Center, Department of Anesthesiology & Pain Medicine; University of Washington, Seattle, Washington, United States of America.

Ethics approval and consent to participate

The study protocol and experiments were approved by the Animal Ethics Committee of Anhui University of Chinese Medicine, Anhui University of Chinese Medicine, Hefei, Anhui, China.

Funding

This work was supported by Opening Project of Zhejiang Provincial Preponderant and Characteristic Subject of Key University (Traditional Chinese Pharmacology), Zhejiang Chinese Medical University（No. ZYAOXZD2019005）（National Key Research and Development Project（RD19100084）, Outstanding Young Talents Project of Universities in Anhui Province Study Abroad（gxgwfx2018043）, Anhui Province Natural Science Foundation (1708085MH196) and the National Natural Science Foundation of China (No. 81102811).

Availability of data and materials

The data sets used during the current study are available from the corresponding author on reasonable request.

References

1. Wang DJ. The prevalence of cardiovascular and cerebrovascular diseases and their main influencing factors. Preventive Medicine Forum. 2016;22:71–5.
2. Lu XY, Xu H, Zhao T, Li G. Study of Serum Metabonomics and Formula-Pattern Correspondence in Coronary Heart Disease Patients Diagnosed as Phlegm or Blood Stasis Pattern Based on Ultra Performance Liquid Chromatography Mass Spectrometry. Chin J Integr Med. 2018;24:905–11.
3. Ma XJ, Yin HJ, Chen KJ. Differential gene expression profiles in coronary heart disease patients of BSS in traditional Chinese medicine and clinical role of target gene. Chin J Integr Med. 2009;15:101–6.
4. Liu H, Zhang WJ, Long CF, Su WW. Protective effects of traditional Chinese herbal formula Compound Xueshuantong Capsule (CXC) on rats with blood circulation disorders. Biotechnol Biotechnol Equip. 2017;31:1–9.
5. Jian WX, Chen QH, Huang XP. Metabolomics study of the myocardial tissue of rats of cardiac blood stasis syndrome. Zhongguo Zhong Xi Yi Jie He Za Zhi. 2012;32:515–20.

6. Cao D, Xu C, Xue Y, Ruan Q, Yang B, Liu Z, Cui H, Zhang L, Zhao Z, Jin J. The therapeutic effect of Ilex pubescens extract on blood stasis model rats according to serum metabolomics. Ethnopharmacolx. 2018;227:18–28.
7. Jatoi SA, Kikuchi A, Gilani SA, Watanabe KN. Phytochemical, pharmacological and ethnobotanical studies in mango ginger (Curcuma amada Roxb.; Zingiberaceae). Phytother Res. 2007;31:56–62.
8. Gunathilake KDPP, Rupasinghe HPV. Recent perspectives on the medicinal potential of ginger. Botanics. 2015;5:55–63.
9. Fang P, Tao QF, Wu XM, Dou H, Shawn S, Mang CY, Xu L, Sun LL, Zhao Y, Li HB, Zeng S, Liu G, Hao XJ. Cytotoxic, cytoprotective and antioxidant effects of isolated phenolic compounds from fresh ginger. Fitoterapia. 2012;83:568–85.
10. Shareef HK, Muhammed HJ, Hussein HM, Hameed IH. Antibacterial effect of ginger (Zingiber officinale Roscoe) and bioactive chemical analysis using gas chromatography-mass spectrometry. Oriental J Chem. 2016;32:817–37.
11. Tohma H, İlhami Gülçin İ, Bursal E, Gören AC, Alwasel SH, Köksa E. Antioxidant activity and phenolic compounds of ginger (Zingiber Officinale Rosc.) determined by HPLC-MS/MS. J Food Meas Char. 2017;11:556–66.
12. Singh G, Kapoor IPS, Singh P, Heluani CSde L, MPde, Catalan CAN. Chemistry, antioxidant and antimicrobial investigations on essential oil and oleoresins of Zingiber officinale. Food Chem Toxicol. 2008;46:3295–302.
13. Brahe LK, Astrup A, Larsen LH. Can we prevent obesity-related metabolic diseases by dietary modulation of the gut microbiota. Adv Nutr. 2016;7:90–101.
14. Ezzat SM, Ezzat MI, Okba MM, Menze ET, Abdel-Naim AB. The hidden mechanism beyond ginger (Zingiber officinale Rosc.) potent in vivo and in vitro anti-inflammatory activity. Ethnopharmacol. 2018;214:113–23.
15. Lee SH, Cekanova M, Baek SJ. Multiple mechanisms are involved in 6-gingerol-induced cell growth arrest and apoptosis in human colorectal cancer cells. Mol Carcinog. 2008;47:197–208.
16. Lee JO, Kim N, Lee HJ, Moon JW, Lee SK, Kim SJ, Kim JK, Park SH, Kim HS. 6-Gingerol affects glucose metabolism by dual regulation via the AMPKα2-mediated AS160–Rab5 pathway and AMPK-mediated insulin sensitizing effects. J Cell Biochem. 2015;116:1401–10.
17. Fang WT, Zhan ZL, Peng HS, Huang LQ. The evolution and changes of the differentiation of dried ginger, ginger and ginger. China Journal of Chinese Materia Medica. 2017;42:1641–5.
18. He SL, Zhong R, Zhao W, Li XB, Li WR, Mi HQ, Wang NS. Effects of Pericarpium Citri Reticulatae and Rhizoma Zingiberis extracts on hemarheology and platelet aggregation of blood stasis model rats. Pharmacology Clinics of Chinese Materia Medica. 2012;28:11–4.
19. Jia DB, Yu M, Li NM, Tang LM, Zhu Y, Li CJ, Liu S, Gong YX, Wei B. Effects of Shenjiangsuoyangyiqi tablets on blood rheology and vascular endothelial function in blood stasis due to cold accumulation and stagnation of the circulation of vital energy model rats. Lishizhen Med Mater Med Res. 2014;25:2347–8.

20. Han YQ, Li YX, Wang YZ, Gao JR, Xia LZ, Hong Y. Comparison of fresh, dried and stir-frying gingers in decoction with BSS in rats based on a GC–TOF/MS metabolomics approach. J Pharm Biomed Anal. 2017;129:339–49.
21. You WH, Wang P, Li MQ, Zhang Y, Peng YL, Zhang FL. Therapeutic effects of modified Danggui Sini Decoction on plasma level of advanced glycation end products in patients with Wagner grade 0diabetic foot: a randomized controlled trial. Zhong Xi Yi Jie He Xue Bao. 2009;7:622–8.
22. Chen E, Lu J, Chen D, Zhu D, Wang Y, Zhang Y, Zhou N, Wang J, Li J, Li L. Dynamic changes of plasma metabolites in pigs with GalN-induced acute liver failure using GC-MS and UPLC-MS. Biomed Pharmacother. 2017;93:480–9.
23. Sasada S, Miyata Y, Tsutani Y, Tsuyama N, Masujima T, Hihara J, Okada M. Metabolomic analysis of dynamic response and drug resistance of gastric cancer cells to 5-fluorouracil. Oncol Rep. 2013;29:925–31.
24. Huang HM, Wu JX, Lu RG, Liu X, Chin BN, Zhu HJ, Yin CY, Cheng B, Wu Z, Chen XJ, Liang YH, Song H, Zheng H, Guo HW, Su ZH. Dynamic urinary metabolomics analysis based on UHPLC-Q-TOF/MS to investigate the potential biomarkers of blood stasis syndrome and the effects of Danggui Sini decoction. Journal of Pharmaceutical and Biomedical Analysis. 2020;179.
25. Wu YZ, Fu Q, Yan QN, Li ZL. Research progress on pharmacological actions of gingerols in cardiovasular disease. Chinese Journal of Clinical Pharmacology. 2017;248:1824–7.
26. Tang YF, Zhang YB, Wang CH, Sun ZG, Li LF, Cheng SQ, Zhou WP. Overexpression of PCK1 Gene Antagonizes Hepatocellular Carcinoma Through the Activation of Gluconeogenesis and Suppression of Glycolysis Pathways. Cell Physiol Biochem. 2018;47:344–55.
27. Ramirez J. ·Periyakaruppan A,·Sarkar S,·Ramesh GT,·Sharma, SC. Effect of Simulated Microgravity on the Activity of Regulatory Enzymes of Glycolysis and Gluconeogenesis in Mice Liver. Microgravity Sci Technol. 2014;25:303–9.
28. Ou DQ, Zeng XD, Liu YH, Liu YY. Advances in the regulation of g-protein-coupled receptor signaling pathway by radix glycyrrhizae. Chin Pharm J. 2012;47:245–9.
29. Chen WQ, Huang XB, Wang NQ, Chen YJ. Effects of paired application of tangerine peel pinellia on the expression of phosphatidylinositol 3 kinase and phosphorylated protein kinase B in rabbits with carotid atherosclerosis. Chin J Cerebrovasc Dis J. 2014;11:364–7,370.
30. Zhang JJ, Deng JT, Shen HQ, Jiang LL, He QW, Zhan J, Zhang ZZ, Wang YL. Pyruvate Protects Against Intestinal Injury by Inhibiting the JAK/STAT Signaling Pathway in Rats With Hemorrhagic Shock. Journal of surgical research. 2020;248:98–108.

Figures

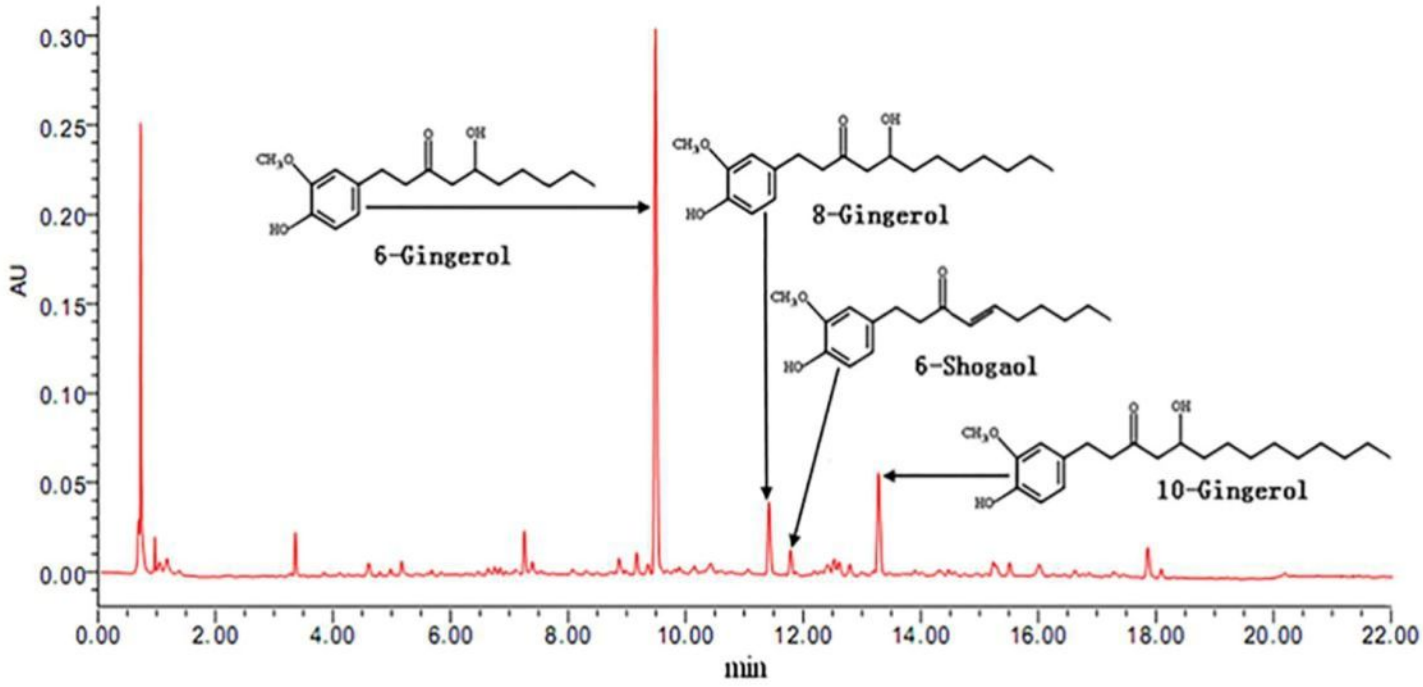

Figure 1

Content determination of 6-gingerol, 8-gingerol, and 10-gingerol in the DG extract.

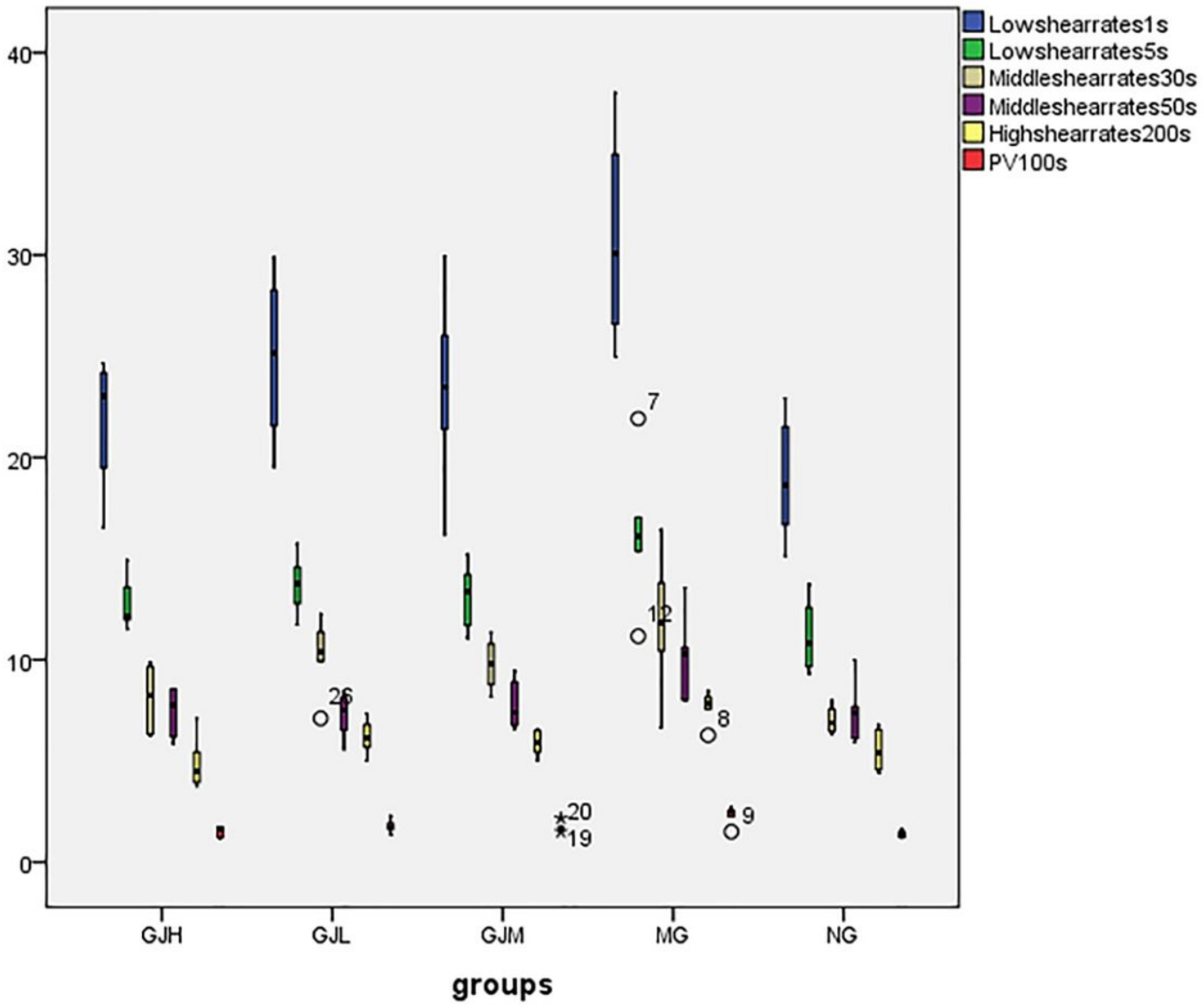

Figure 2

Box - whisker plot of effects of different shear rates on WBV (mPa•s) in each group. The WBV of the MG of BSS increased significantly at all shear rates and the MG had a significantly higher plasma viscosity than that of each group.

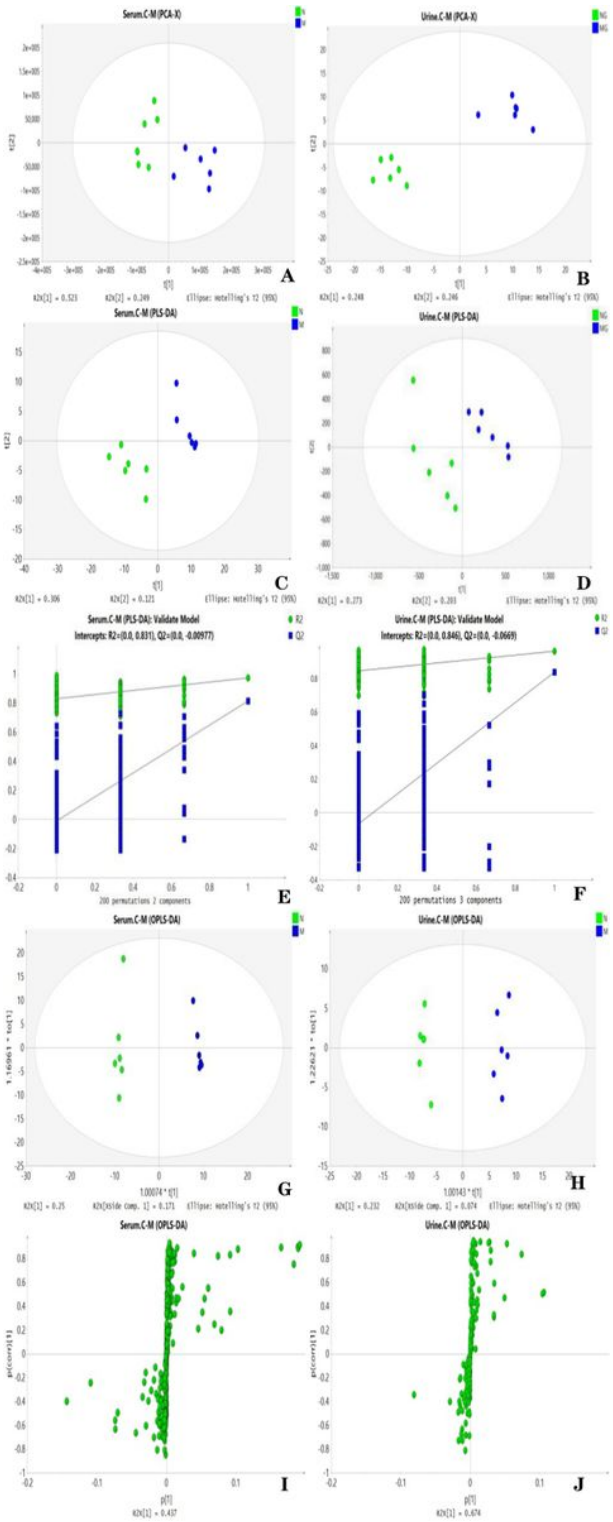

Figure 3

Score plots from the PCA model of the NG vs. the MG for (A) serum and (B) urine and PLS-DA model of the NG vs. the MG for (C) serum and (D) urine . Two hundred permutations of the PLS-DA model for serum (E) and urine (F). Score plots form the OPLS-DA model of the CG vs. the MG for serum (G) and urine (H). S-Plots from the OPLS-DA model for serum (I) and urine (J).

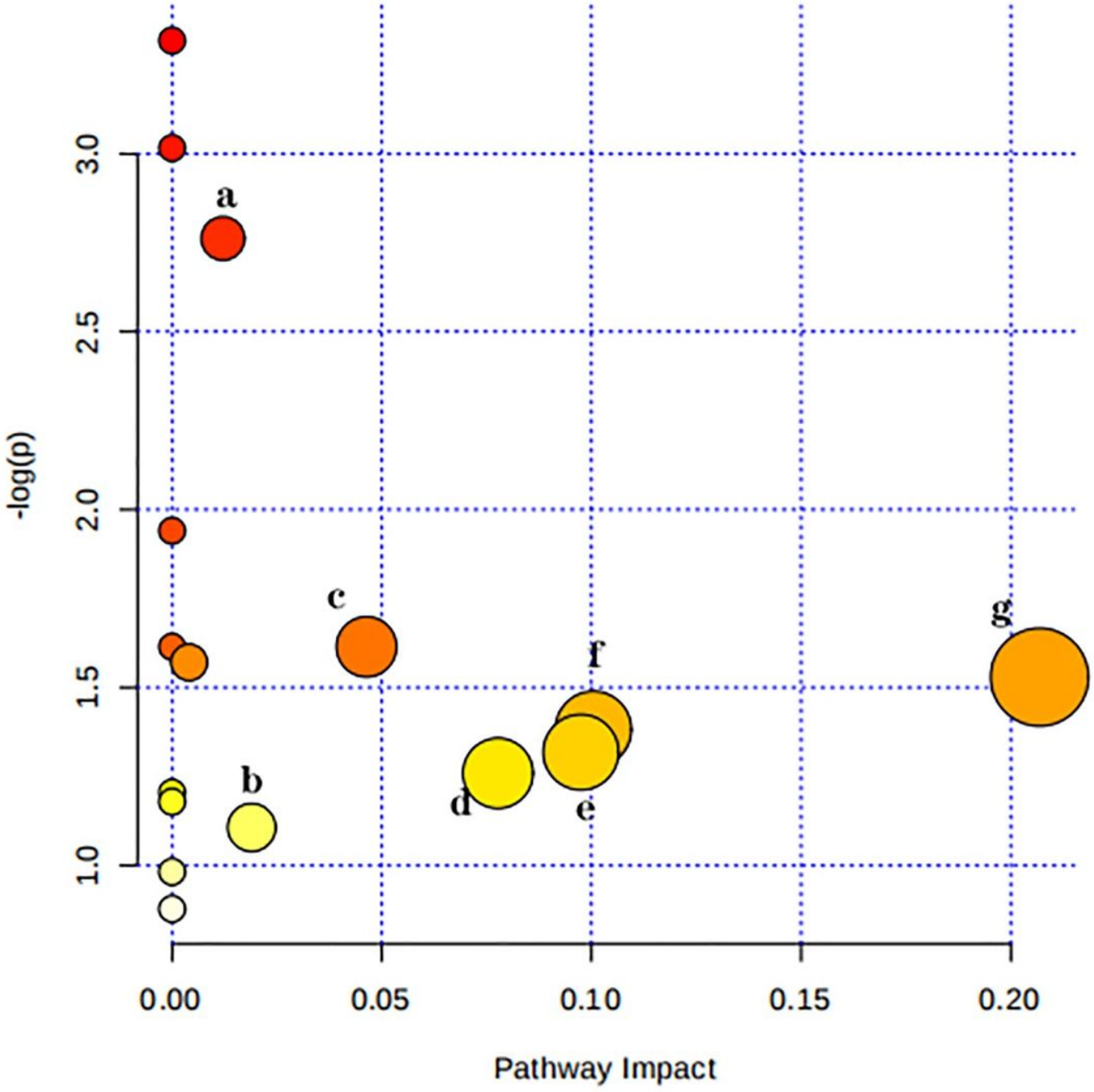

Figure 4

Summary of pathway analysis of serum and urine samples of the blood stasis rats. (a) Arginine and proline metabolism ; (b) Glycerophospholipid metabolism; (c) Citrate cycle (TCA cycle); (d) Inositol phosphate metabolism; (e) Glycolysis / Gluconeogenesis ; (f) Phosphatidylinositol signaling system; (g) Pyruvate metabolism.

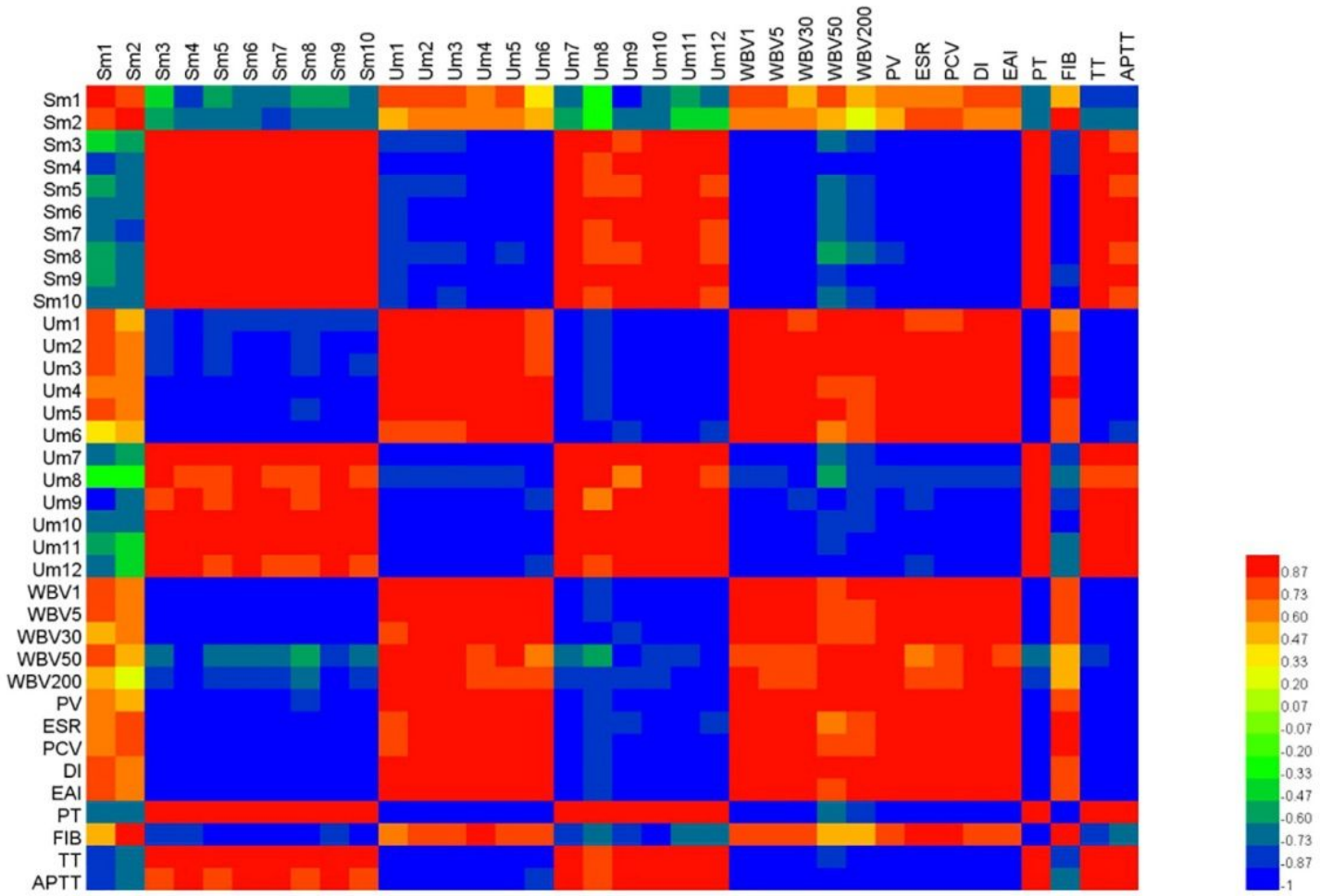

Figure 5

Correlation map of rat serum and urine metabolites and pharmacodynamics indices according to Pearson's correlation coefficients. Degrees of correlation degrees are shown using a color scale from significantly negatively correlated (blue) to significantly positively correlated (red).

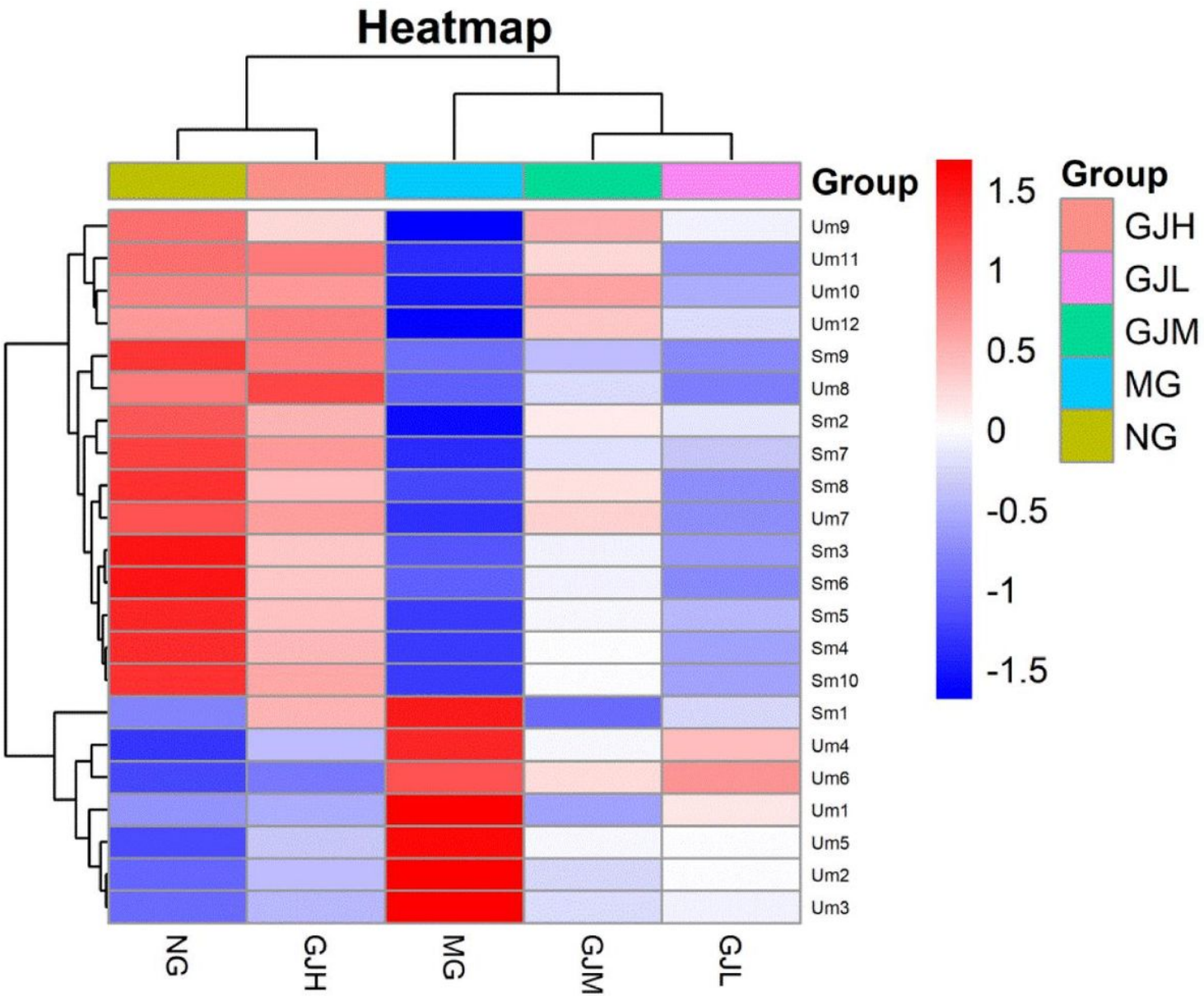

Figure 6

Heat map analysis of different groups of metabolites (with the deepening of red, the expression level of endogenous substances gradually increased, and with the deepening of blue, the expression level of endogenous substances gradually decreased).

Supplementary Files

This is a list of supplementary files associated with this preprint. Click to download.

- Additionalfile1.doc
- Additionalfile2.doc